Available online at www.sciencedirect.com
ScienceDirect
Journal of Power Sources 163 (2007) 768–776
JOURNAL OF POWER SOURCES
www.elsevier.com/locate/jpowsour

Current distribution measurements with a free-breathing direct methanol fuel cell using PVDF-*g*-PSSA and Nafion®117 membranes

V. Saarinen [a,*], O. Himanen [b], T. Kallio [a], G. Sundholm [a], K. Kontturi [a]

[a] *Helsinki University of Technology, Laboratory of Physical Chemistry and Electrochemistry, P.O. Box 6100, 02015 TKK, Finland*
[b] *Helsinki University of Technology, Laboratory of Advanced Energy Systems, P.O. Box 2200, 02015 TKK, Finland*

Received 6 April 2006; received in revised form 25 August 2006; accepted 12 September 2006
Available online 13 November 2006

Abstract

The methanol crossover and other mass transfer phenomena have been investigated in a free-breathing direct methanol fuel cell (DMFC). The current distribution profile along the MeOH flow channel was measured and information of local concentrations of the reacting species was obtained. The DMFC with a segmented cathode was found to be very useful for a detailed analysis of the interrelated parameters, which cause the local variations of the cell current. The connections between different operating parameters were clarified in detail for two different membranes. The measurements were done for both an experimental poly(vinylidene fluoride)-*graft*-poly(styrene sulfonic acid) (PVDF-*g*-PSSA) membrane and the commercial Nafion®117 membrane, which have different methanol permeabilities. The MeOH concentration and the flow rate were varied in a wide range in order to determine their optimum values. The deviations from an even current density distribution were observed to increase as a function of MeOH concentration and decrease as a function of temperature. The power production of a free-breathing DMFC was observed to be proportional to the local oxygen concentration at the cathode side and inadequate air convection together with the MeOH crossover phenomenon was observed to decrease the cell performance locally.

Keywords: DMFC; Current distribution; Free-breathing segmented cathode; PVDF-*g*-PSSA; Methanol crossover

1. Introduction

The direct methanol fuel cell (DMFC) is a polymer electrolyte fuel cell (PEFC), where the anode reactant is a liquid mixture of methanol and water. The use of methanol gives some advantages compared to the hydrogen systems: the storage of fuel is easier and the systems can have a simpler structure. Methanol has a higher energy density than hydrogen, according to Ref. [1]: MeOH: 17×10^9 J m^{-3} (100 wt.%, 25 °C), H_2: 0.6×10^9 J m^{-3} (6.9×10^6 Pa, 25 °C). Because of simplicity, space saving and economical reasons, some applications of DMFC (e.g. portable electronics) will probably be so-called passive-feed DMFC, completely free-breathing without any external pumps.

In order to achieve optimum performance values for the DMFC, it is important to have an even current and temperature distribution inside the fuel cell. This can be achieved, when the concentrations of the reactants have optimum values. In many cases the goal of the fuel cell development is also to achieve an even current density profile under a variety of operating conditions. As a consequence, current distribution measurements are very valuable for the better understanding of the complex relationships between different variables and operating parameters of the DMFC. The areal variations of the cell current give information on local concentrations of reacting species and mass-transfer phenomena, which are occurring inside the fuel cell. During recent years, current distribution measurements have been used in many PEFC [2–11] and DMFC [12–15] studies and various experimental techniques have been developed.

A printed circuit board approach with segmented current collector and flow field has been used by Cleghorn et al. [2] and a partial membrane electrode assembly (MEA) method, where the active cathode area was varied, by Stumper et al. [3]. Wieser et al. [4] used a magnetic loop current sensor approach (Hall sensors) and Eckl et al. [11] a segmented bipolar plate approach. In most of the studies the cathode has been segmented, but sometimes the anode [8,9]. Gülzow et al. [12] have studied differences in different MEAs (originating from the manufacturing process) with a segmented DMFC (16 segments) and Geiger et al. [15] have also

* Corresponding author. Tel.: +358 50 5259669; fax: +358 94512580.
E-mail address: vss@cc.hut.fi (V. Saarinen).

0378-7753/$ – see front matter © 2006 Elsevier B.V. All rights reserved.
doi:10.1016/j.jpowsour.2006.09.016

made segmented DMFC measurements (9 segments) concluding that the current distribution is highly dependent on the O_2 concentration. The current distribution can also be analyzed with other data, e.g. localized impedance measurements [16], water distribution measurements [14] or distribution measurements of gaseous species (H_2O, H_2, O_2, N_2) [10]. In the catalyst studies, the array MEAs have been used as catalyst screening devices [13] and for the analysis of the local catalyst poisoning [17].

In the case of the DMFC, the methanol crossover (methanol permeability through the membrane) is a very dominating phenomenon [18] and it has been investigated widely [19–30]. However, most of these studies have been done without current distribution measurements. The methanol permeated from anode to cathode poisons the Pt catalyst and causes mixed potentials, which decrease the fuel cell performance [31,32]. The DMFC with a segmented cathode can provide very detailed information on the concentrations of reacting species, in which part of the DMFC most of the current is produced and how much the MeOH crossover phenomenon decreases the cell performance locally. All of those phenomena are not seen, if only the total cell current is measured. From the engineering aspect, it is possible to see with a segmented DMFC, how the different MeOH flow rates affect cell performance and what is the lowest adequate MeOH flow rate (and stoichiometry), for which the performance of the DMFC is not yet MeOH mass-transfer limited. From the theoretical aspect, many fuel cell models [33–35] have been developed during recent years, but most of the model validations have only been done with polarization curves [35]. The current distribution data could also be useful for the verification of the fuel cell models.

In this study, the main goal was to investigate the mass-transfer phenomena and especially MeOH crossover in the DMFC. Also, the connection between MeOH concentration and flow rate was studied in order to find their optimum values. During the measurements, the DMFC was operated with free air convection at the cathode side. The cathode flow field plate was divided into 48 segments and the current distribution was measured with a resistor network. Similar approach has been used in PEFC studies by Noponen et al. [5,6]. The current distribution measurements were done as a comparative study between an experimental poly(vinylidene fluoride)-*graft*-poly(styrene sulfonic acid) (PVDF-*g*-PSSA) membrane and the commercial Nafion®117 membrane. These membranes were selected, since they have different performance values and MeOH crossover rates in the DMFC. The Nafion®117 membranes have been used widely in DMFC studies [12,19–21,23,27,36–38] and they have the lowest MeOH crossover rate of the commonly used Nafion® membranes [38]. The experimental PVDF-*g*-PSSA membrane has been characterizated with other methods in previous studies [28,39–41].

2. Experimental

2.1. The segmented free-breathing DMFC

The current distribution measurements were done with a segmented free-breathing direct methanol fuel cell and the flow field plates used are presented in Fig. 1. The cell was aligned so that there was a free vertical convection of air upwards in the cell. The measurement system is slightly modified from the one, which is described in detail elsewhere [5]. In this study the cell was used as a DMFC, whereas in Ref. [5] the fuel cell was used as a PEFC with a hydrogen feed. Also the used membrane electrode assemblies were different and the anode flow field plate was designed to be convenient for the DMFC measurements. During the measurements the MeOH solution was pumped to the anode with a Reglo-CPF pump (Ismatec). The anode flow channel geometry was serpentine and the MeOH flow direction was mainly vertical. The cathode segments were located between two parallel serpentine flow channels. With that disposition the current density variations can be studied along the MeOH flow channel. The anode channel is illustrated in Fig. 2 and the locations of the cathode segments are also shown in the same figure. The MeOH solution was pumped into the flow channel from the bottom left corner and outflow was from the bottom right corner.

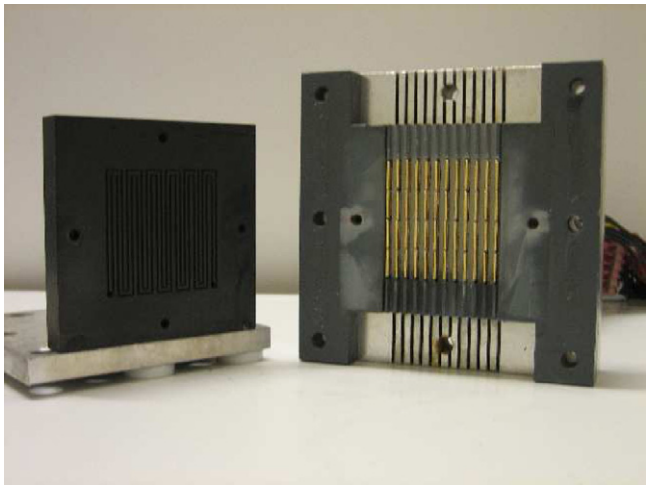

Fig. 1. The DMFC anode flow field plate (left) and the segmented free-breathing cathode (right).

The cathode flow field plate was segmented in 48 pieces: 4 horizontal rows and 12 segments in every row. The segmentation was not extended to the gas diffusion layer (GDL), only the current collector was segmented. Noponen et al. [5] also estimated and modeled the effect of a non-segmented GDL and concluded that the current density distribution can be measured with reasonable accuracy, even if the GDL is not segmented. The segments were made of gold plated stainless steel and their contact force against the GDL could be individually adjusted. Every current collector pin was connected to a 0.1 Ω resistor. The current density values $i_{i,j}$ can be then calculated according to Eq. (1) from the voltage values $u_{i,j}$, which were measured over the resistors:

$$i_{i,j} = \frac{u_{i,j}}{a_{i,j}R} \tag{1}$$

where $i_{i,j}$ is the local current density, $u_{i,j}$ the measured voltage over the corresponding resistor, $a_{i,j}$ the effective area of the segment and R is the resistance. Subscripts i and j refer to the placement of the current collector pin. It was assumed that the effective sizes of each segments were equal ($a_{i,j} = 25\,\text{cm}^2/48$

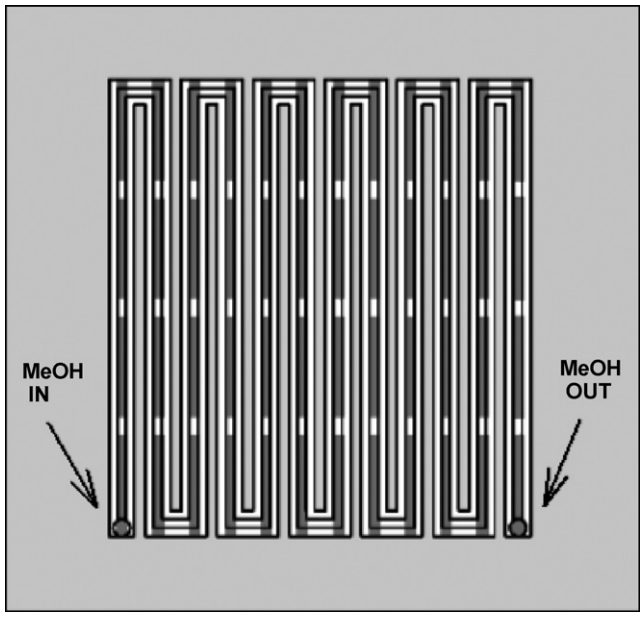

Fig. 2. The anode flow field plate and the locations of the cathode segments.

$\approx 0.52\,cm^2$). This was not exactly true, since the effective areas of the segments were slightly smaller near the edges of the cell. Also, the contacts between the pins and the GDL were not exactly equal, even though they were adjusted to be as equal as possible.

The voltage drops over the resistors were measured with HP34901A multiplexer cards connected to a HP34970A data logger. During the measurements the cell was operated at steady state conditions (in constant current mode) and since only one channel was measured at a time (measurement time was about 0.1 s), it took approximately 5 s to measure all the segments once. The 5 s measurement sequence was followed by a 10 s rest period and the current distributions were calculated as a mean value of at least 10 sequences.

2.2. Membranes and electrodes

The PVDF-*g*-PSSA membrane was made of poly(vinylidene fluoride) film by an irradiation method followed by grafting with styrene monomers. Then the film was sulfonated in chlorosulfonic acid/dichloroethane solution. A tentative chemical structure of the PVDF-*g*-PSSA membrane is presented in Fig. 3. The manufacturing process and the main properties of the PVDF-*g*-PSSA membrane are described in more detail elsewhere [28,39–41]. The PVDF-*g*-PSSA membrane was soaked in ion exchanged water before the hot-pressing of the MEA.

The Nafion®117 membrane was pretreated before hot-pressing by boiling it 0.5–1 h in a 5% H_2O_2 solution, then boiling it three times for 0.5–1 h in ion exchanged water, then 0.5– 1 h

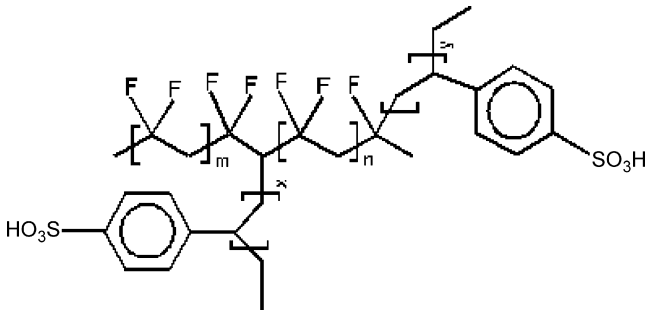

Fig. 3. A tentative chemical structure of the PVDF-*g*-PSSA membrane.

in 0.5 M H_2SO_4 and finally again three times for 0.5–1 h in ion exchanged water. The main properties of the PVDF-*g*-PSSA and the Nafion®117 membranes are presented in Table 1. Conductivities of the examined membranes were of the same magnitude, but Nafion®117 was much thicker than PVDF-*g*-PSSA. In this study, the degree of grafting (DOG) of PVDF-*g*-PSSA was 39%. Even higher conductivity values (up to 8.0 S m^{-1} at 20 °C) have been reported [39] for PVDF-*g*-PSSA with higher DOG values, but then the stability of the membrane in the fuel cell decreases. Kallio et al. [28] have measured MeOH diffusion coefficients in PVDF-*g*-PSSA, which were about 30% of the corresponding values of Nafion®115 ($l = 130$ μm) in a temperature range of 30–70 °C. On the other hand, since the PVDF-*g*-PSSA membrane was about 50% thinner than the Nafion®115 membrane, almost equal MeOH permeation rates have been measured through these membranes [28]. As a consequence, since Nafion®117 is 50 μm thicker than Nafion®115, the MeOH permeation rate through PVDF-*g*-PSSA is somewhat higher than through Nafion®117.

The electrodes ($A = 25\,cm^2$) were commercial gas diffusion electrodes (E-TEK): cathode: 2.0 mg cm^{-2} Pt Black, anode: 2.0 mg cm^{-2} [Pt–Ru]Ox unsupported. Before hot-pressing the electrodes were coated with a Nafion solution (0.5–0.8 mg cm^{-2}) (Aldrich) and kept in 0.5 M H_2SO_4 for 12 h in order to exchange the Nafion coating into protonic form. After the pretreatment the MEAs were hot-pressed: PVDF-*g*-PSSA: 120 s 100 kPa 120 °C, Nafion®117: 120 s 100 kPa 140 °C.

2.3. Measurement parameters: theoretical and practical aspects

The governing electrochemical reactions in the DMFC are

$$\frac{3}{2}O_2 + 6H^+ + 6e^- \longrightarrow 3H_2O \quad (2)$$

$$CH_3OH + H_2O \longrightarrow CO_2 + 6H^+ + 6e^- \quad (3)$$

Reaction (2) is the main DMFC cathode reaction and resulting from the MeOH crossover phenomenon, the anode reaction (3) will also occur at the cathode. When the MeOH crossover

Table 1
The properties of the examined membranes

	Thickness dry (μm)	Thickness wet (μm)	WU (%)	DOG (%)	IEC (mequiv g^{-1})	σ (25 °C) (S m^{-1})
PVDF-*g*-PSSA	70	90	85	39	2.5	4.5
Nafion®117	180	210	20	–	0.9	5.0

rate through the membrane is low, reaction (2) is dominating at the cathode. But if the MeOH concentration is increased at the anode side, the MeOH crossover rate will also increase. Because of the permeated MeOH and MeOH consumed in anode reactions, there will be a MeOH concentration profile along the flow channel. The shape of this profile also depends on the MeOH flow rate and the membrane properties (MeOH and water uptake, conductivity, etc.). If the DMFC is operated with a relatively high constant current and with a low MeOH concentration and flow rate, most of the MeOH is consumed at the anode. As a consequence, there is only a low amount of MeOH left, which can permeate through the membrane and react at the cathode.

On the contrary, if the DMFC is operated with a low cell current, the MeOH crossover rate will be high. That leads further on to decreased performance values, resulting from the CO poisoning of the cathode catalyst. Also, the incomplete oxidation of methanol and other side reactions will lead to mixed potentials and cause that the measured open circuit voltage (OCV) in the DMFC is much lower than the theoretical value 1.21 V. The cathode Pt catalyst is more vulnerable for CO poisoning than the anode Pt–Ru, where the adsorbed –OH groups on ruthenium enhance significantly CO removal and CO_2 formation [42]. The CO poisoned Pt cathode will remain covered with CO, unless the temperature or potential are raised to cause the thermal desorption or oxidation of CO molecules [31].

High mass transfer overpotentials can exist in a free-breathing DMFC, even at relatively low current densities. That is resulting from an inadequate air flow towards the cathode and a slow evaporation of water, which is produced in reaction (2). The performance values of the DMFC are affected a lot by the cell temperature [36,43] and when it is increased, also the reaction rates at both electrodes will increase. The well-known observation (at temperatures below 100 °C) is that the maximum power densities of the DMFC will increase as a function of temperature, mainly as a result of the increased catalytic activity (decreased activation overpotential). On the other hand, much of this gain is lost by the fact that the MeOH permeability also increases as a function of temperature [28].

In this study, the measurements were done using 0.5, 1, 3, 5 and 10 M MeOH solutions and the MeOH flow rates were also varied in a wide range from 3.3×10^{-9} to 130×10^{-9} $m^3\ s^{-1}$. If a complete MeOH oxidation is assumed at the anode, the MeOH stoichiometry λ can be calculated according to Faraday's law of electrolysis:

$$\lambda = \frac{nF\dot{V}c}{I_{\text{cell}}} \tag{4}$$

where n is the number of electrons (6), F the Faraday's constant, $\dot{V}$ the MeOH flow rate, c the MeOH concentration and I_{cell} is the measured cell current. The MeOH stoichiometry was varied in a wide range from 3 to 2500. As an example, at a current density of 120 A m^{-2} and a flow rate of 3.3×10^{-9} $m^3\ s^{-1}$, the stoichiometries, which correspond to the MeOH concentrations of 0.5, 1, 3, 5 and 10 M are 3, 6, 19, 32 and 64, respectively.

The current distribution measurements were made with both PVDF-*g*-PSSA and Nafion® 117 in similar conditions. Since the used temperature and the cell current affects the MeOH utilization rate and the above mentioned phenomena, the measurements were done at three different cell temperatures (30, 50 and 70 °C) and using different current densities. Most of the current measurements were done using average current densities of 120, 320 and 520 A m^{-2}. Those values were selected, since they were the most suitable to be used at all operating conditions (two membranes, three cell temperatures, five MeOH concentrations, three MeOH flow rates).

3. Results and discussion

3.1. Performance comparison between PVDF-g-PSSA and Nafion® 117 membranes

Generally, when the best performance values were measured, the current density distribution was even. The deviations from that even current density distribution increased as a function of MeOH concentration. Also, since the DMFC was free-breathing, it was observed at higher current densities and especially at lower temperatures that the air (oxygen) convection towards the cathode was inadequate. As a consequence, when the cell was operated with a very high current, almost all of the cell current was produced at the 12 lowest cathode segments. The air convection was inadequate towards the higher segments and very low current density values were measured, especially from the segments near the upper edge.

The polarization curves for PVDF-*g*-PSSA and Nafion® 117 at 30 and 70 °C are presented in Fig. 4 (1 M MeOH, 17×10^{-9} $m^3\ s^{-1}$). Although the proton conductivities of both the examined membranes were quite similar, the measured maximum power densities of PVDF-*g*-PSSA were 20–50% lower than the corresponding values of Nafion® 117. The main reason for that was probably the higher MeOH crossover rate through the PVDF-*g*-PSSA membrane. There were also structural differences between the membranes and it is presumable that the contact between the electrodes and the PVDF-*g*-PSSA membrane was not as good as with Nafion® 117. Both electrodes were coated with Nafion® solution and resulting from the material properties, the maximum hot-pressing temperature for PVDF-*g*-PSSA was only 120 °C.

The open circuit voltage and maximum performance values of PVDF-*g*-PSSA and Nafion® 117 at low MeOH concentrations (0.5–3 M) were more similar than at higher concentrations (5–10 M). That observation validates also that the MeOH crossover rate through the PVDF-*g*-PSSA membrane was higher than through the Nafion® 117 membrane. Only very low average current densities could be used with a MeOH concentration of 5 M or higher. The current density distributions with 5 M MeOH for Nafion® 117 and PVDF-*g*-PSSA at 70 °C are presented in Fig. 5. The average current density was 120 A m^{-2} and a MeOH flow rate was 17×10^{-9} $m^3\ s^{-1}$, which corresponds to the MeOH stoichiometry of 160. The corresponding cell voltages for Nafion® 117 and PVDF-*g*-PSSA were 280 and 50 mV, respectively. Since the cell voltage was higher with Nafion® 117, also the power density was higher and a larger proportion of the current was produced at the lowest segments. When the DMFC was operated with the same parameters except with a

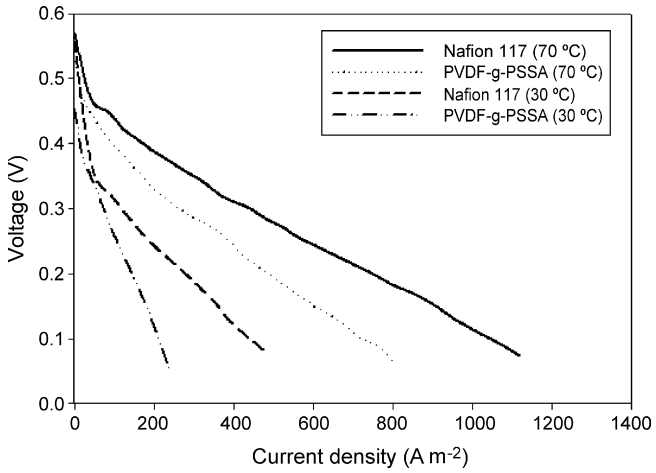

Fig. 4. The polarization curves in the DMFC for PVDF-*g*-PSSA and Nafion® 117 at 30 and 70 °C (1 M MeOH).

lower MeOH concentration, the current distributions were more even and similar for both of the membranes. The difference in the cell voltage was also smaller, e.g. with 1 M MeOH: Nafion® 117: 420 mV, PVDF-*g*-PSSA: 380 mV.

The highest power densities for Nafion® 117 and PVDF-*g*-PSSA were measured with 1 M MeOH solution at all cell temperatures used (30, 50 and 70 °C). The observation concerning Nafion® 117 was similar to what has been reported in other studies [21,36]. When the MeOH concentration was increased to 3 M or higher, the cell performance decreased and that was seen again as a more uneven current distribution. The performance decrease with higher MeOH concentrations was mainly caused by the MeOH crossover phenomenon, which lowers the cell voltage and with the segmented DMFC this can also be observed as a change in the shape of the current distribution. An example of performance decrease is presented in Fig. 6: two current density distributions for the Nafion® 117 membrane at 70 °C. When the MeOH concentration was 0.5 M, the current distribution was very even, whereas with a 10 M MeOH solution, most of the cell current was produced at the lowest segments. During those measurements, the DMFC was operated with an average current density of 120 A m^{-2} and a MeOH flow rate of 17×10^{-9} m^3 s^{-1}. The MeOH stoichiometries for 0.5 and 10 M MeOH were 16 and 320, respectively. When the MeOH concentration was increased from 0.5 to 10 M, the cell voltage decreased from 540 to 150 mV.

The lowest adequate MeOH stoichiometry, for which the performance of the DMFC was no longer MeOH mass-transfer limited, was also measured at different temperatures. In most cases, a MeOH flow rate of 17×10^{-9} m^3 s^{-1} was high enough to give good performance values. Increasing the stoichiometry above 5 was useful only, when the DMFC was operated at very high current densities.

3.2. The effects of MeOH concentration and stoichiometry

During the measurements, the DMFC with a segmented cathode was found to be a very convenient tool for investigation of areal relations between the MeOH concentration and the flow rate. An example: when the current distribution measurements were done for the PVDF-*g*-PSSA membrane with an average current density of 320 A m^{-2} at 70 °C, the cell voltage variations depending on the MeOH flow rate, were for 1 and 3 M MeOH solution 190–260 and 20–270 mV, respectively. The highest voltage values were measured at flow rates of 17×10^{-9} m^3 s^{-1} (1 M MeOH) and 3.3×10^{-9} m^3 s^{-1} (3 M MeOH). The measured current density distributions for 1 M MeOH with flow rates of 3.3×10^{-9} and 17×10^{-9} m^3 s^{-1} are presented in Fig. 7. When the flow rate was 3.3×10^{-9} m^3 s^{-1}, which corresponds to a stoichiometry of 2.4, it was clearly seen that MeOH was running out in the end of the flow channel. There was a decreasing current density profile towards the MeOH outflow (bottom right corner) in a horizontal direction (from left to right). Whereas with a flow rate of 17×10^{-9} m^3 s^{-1}, which corresponds to a stoichiometry of 12, the current distribution was even and good performance values were measured. When the MeOH flow rate with 1 M MeOH was increased from 17×10^{-9} to 130×10^{-9} m^3 s^{-1} (to a stoichiometry of 96) no remarkable changes were observed in the current distribution.

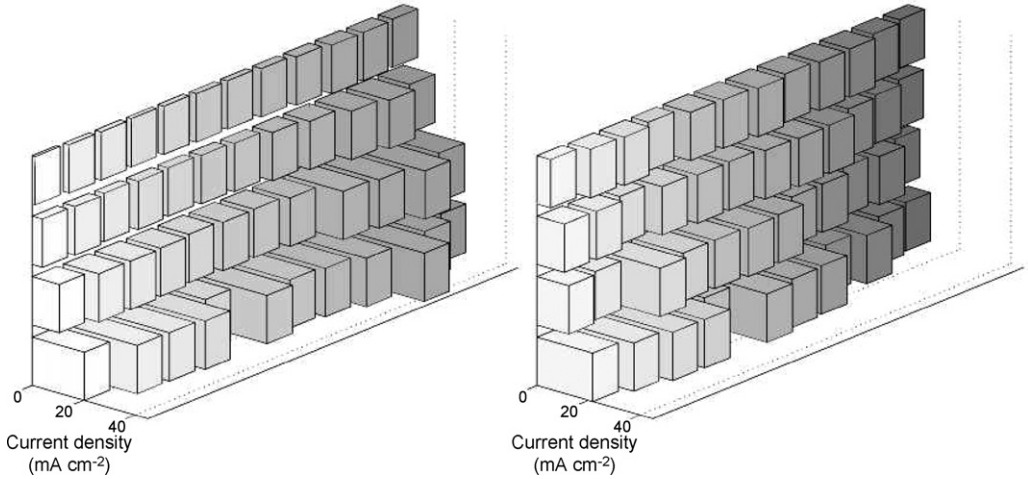

Fig. 5. The measured current distributions for Nafion® 117 (left) and PVDF-*g*-PSSA (right) with an average current density of 120 A m^{-2} at 70 °C. The MeOH concentration was 5 M and the flow rate 17×10^{-9} m^3 s^{-1}.

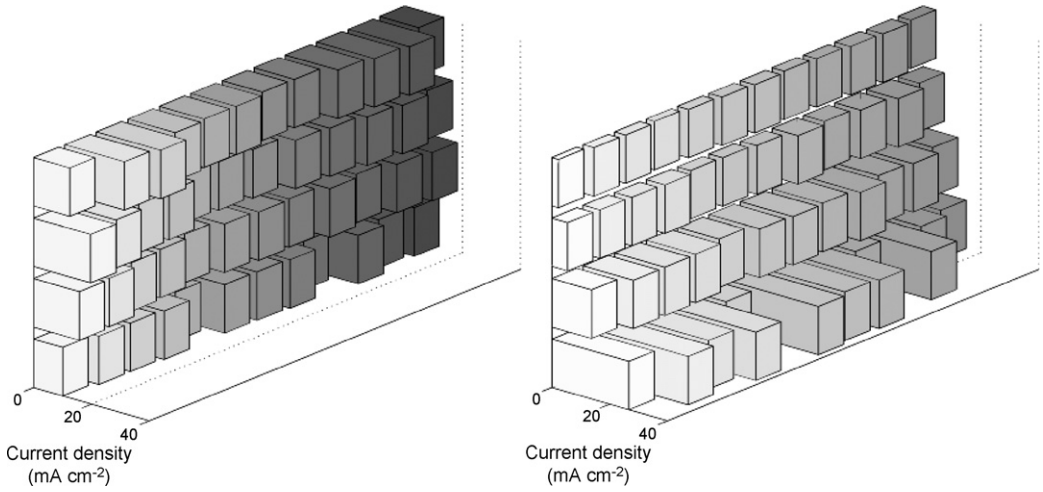

Fig. 6. The measured current density distributions for the Nafion®117 membrane with an average current density of 120 A m^{-2} at 70 °C, MeOH flow rate was 17×10^{-9} m^3 s^{-1} and concentrations 0.5 M (left) and 10 M (right).

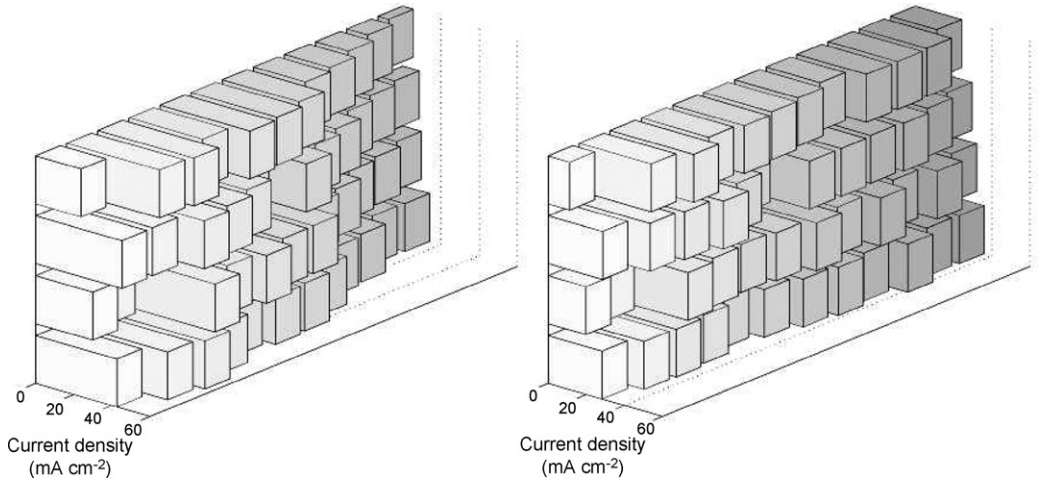

Fig. 7. The measured current density distributions for the PVDF-*g*-PSSA membrane with an average current density of 320 A m^{-2} at 70 °C: flow rates of 1 M MeOH: 3.3×10^{-9} m^3 s^{-1} (left) and 17×10^{-9} m^3 s^{-1} (right).

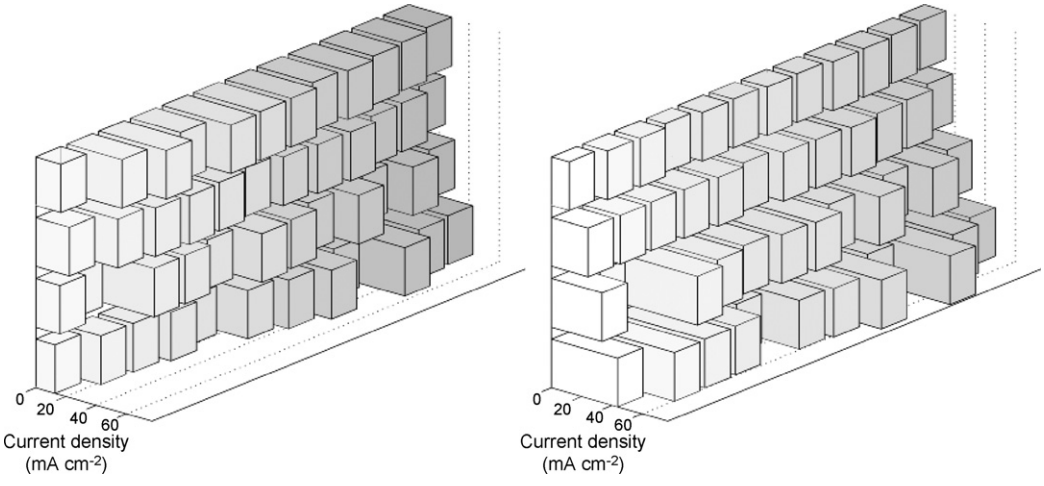

Fig. 8. The measured current density distributions for the PVDF-*g*-PSSA membrane with an average current density of 320 A m^{-2} at 70 °C: flow rates of 3 M MeOH: 3.3×10^{-9} m^3 s^{-1} (left) and 17×10^{-9} m^3 s^{-1} (right).

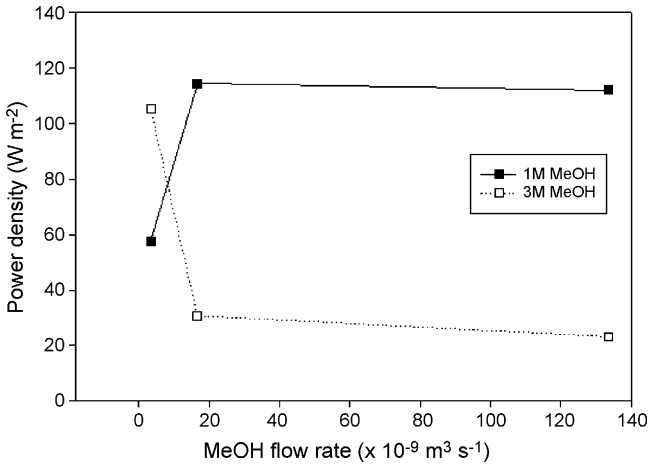

Fig. 9. The measured maximum power densities for the PVDF-*g*-PSSA membrane at 70 °C.

An example of current distribution measurement, where a relatively low MeOH flow rate was combined with relatively high MeOH concentration, is presented in Fig. 8. The comparison between current distributions in Fig. 8 is similar to that in Fig. 7, but now the MeOH concentration is 3 M instead of 1 M. In the case of the flow rate of 3.3×10^{-9} m^3 s^{-1}, which corresponds to the total stoichiometry of 7, the contrary behavior than with 1 M MeOH was observed: the current densities increased along the MeOH flow channel and the highest current densities were located at the very end of the MeOH flow channel. This can be explained with the decrease of MeOH concentration. The electrochemical oxidation of MeOH takes place and due to the low MeOH flow rate, the MeOH solution diluted and its concentration approached the optimum value towards the end of the flow channel. Resulting from the decreased MeOH concentration, also the MeOH crossover rate was lower at the end of the flow channel.

When the flow rate of 3 M MeOH was increased from 3.3×10^{-9} to 17×10^{-9} m^3 s^{-1} (to a stoichiometry of 36), the cell voltage decreased over 200 mV and a steep decrease in current densities was observed in a vertical direction. Most of the current was produced at the 12 lowest cathode segments. This can be explained again with the MeOH crossover and a limited oxygen mass-transport to the cathode. When the flow rate with 3 M MeOH was increased from 17×10^{-9} to 130×10^{-9} m^3 s^{-1} (to a stoichiometry of 290), the decrease in current densities in a vertical direction was even higher, but the shape of the current distribution was still the same.

The measured maximum power densities for the PVDF-*g*-PSSA membrane with 1 and 3 M MeOH feed as a function of MeOH flow rate are presented in Fig. 9. When the MeOH concentration was 1 M or less, the MeOH crossover was minor. At low flow rates, the MeOH stoichiometry was too low for the optimal performance. On the contrary, no significant improvement of maximum power density was obtained at higher flow rates than 17×10^{-9} m^3 s^{-1}. When 3 M MeOH solution was used and the flow rate was low, the MeOH concentration decreased along the flow channel and relatively high power densities were measured. Whereas increasing the flow rate to 17×10^{-9} m^3 s^{-1} or higher, the MeOH crossover became dominating and that was seen as a dramatic decrease in the power density.

During the measurements, it was observed that the current densities can vary significantly inside the DMFC and in some cases even negative currents were measured. This can happen, when the MeOH crossover rate is relatively high and the cell is operated with relatively low current densities. An example of negative cell currents is presented in Fig. 10: two current distributions for the Nafion®117 membrane with an average current density of 120 A m^{-2} at 70 °C . The flow rates of 3 M MeOH were 3.3×10^{-9} and 17×10^{-9} m^3 s^{-1} and the corresponding MeOH stoichiometries were 19 and 96, respectively. At left in Fig. 10, the current densities were negative near the MeOH feed, since the electrochemical oxidation of MeOH according to Eq. (3) was dominating at those cathode segments. In the upper left corner of the same figure, there were two segments next to each other, where the local current densities were about −80 and 80 A m^{-2}. That corresponds to a potential difference

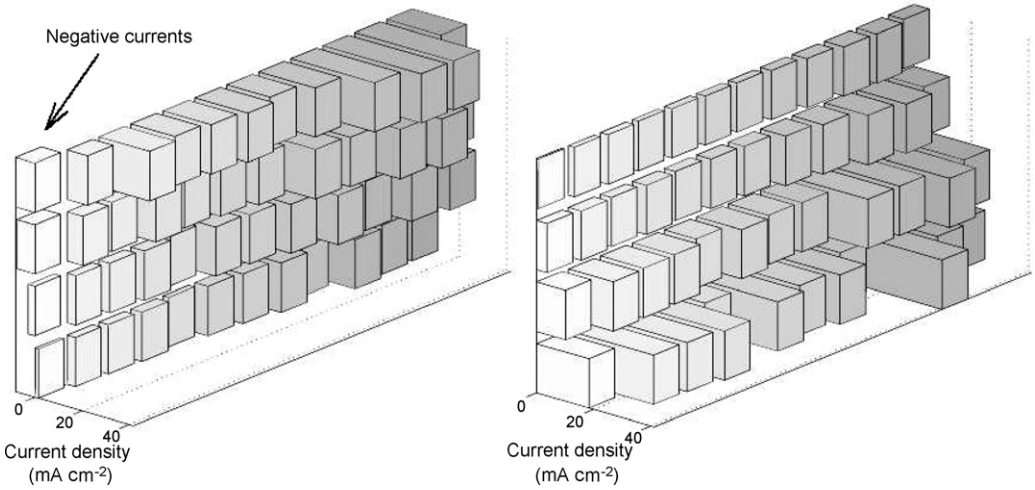

Fig. 10. The measured current density distributions for the Nafion®117 membrane with an average current density of 120 A m^{-2} at 70 °C: flow rates of 3 M MeOH: 3.3×10^{-9} m^3 s^{-1} (left) and 17×10^{-9} m^3 s^{-1} (right).

of 0.8 mV between those segments. Since the actual cell voltage was 510 mV, the corresponding local potentials (after 0.1 Ω resistors) were 509.6 and 510.4 mV. As a general observation, when the local current density values $i_{i,j}$ were calculated according to Eq. (1), the differences between measured local potential values $u_{i,j}$ were typically about 1–3 mV.

In the case of MeOH flow rate of 3.3×10^{-9} m^3 s^{-1} (at left in Fig. 10), the currents increased along the flow channel. Resulting again from the low MeOH flow rate, MeOH concentration decreased and approached an optimum value towards the end of the flow channel. The cell voltage decreased from 510 to 360 mV, when a MeOH flow rate was increased from 3.3×10^{-9} to 17×10^{-9} m^3 s^{-1}. In the latter case, the MeOH flow rate and stoichiometry were so high that no remarkable decrease of concentration happened along the flow channel. As can be seen at right in Fig. 10, most of the current was produced at the 12 lowest cathode segments and there was a steep decrease of current densities in a vertical direction. The shape of that current distribution was quite similar to what was measured for PVDF-*g*-PSSA (presented at right in Fig. 8). When similar measurements as in Fig. 10 were done with using an average current density of 520 A m^{-2} instead of 120 A m^{-2}, the shapes of the current distributions were quite similar, except that the currents remained also positive near the MeOH input. This indicates that the higher MeOH utilization at the anode side decreases the influence of MeOH crossover.

4. Conclusions

The DMFC with a segmented cathode current collector can be used effectively for finding the parameters for the best fuel cell performance and an optimal MeOH utilization (stoichiometry). Since the power production of the free-breathing DMFC is proportional to the oxygen concentration at the cathode side, inadequate air convection leads to uneven current distribution. Especially with low cell voltages, the mass-transport to the cathode was dominating and that was seen during the current distribution measurements as a steep decrease in current densities in a vertical direction: most of the current was produced at the 12 lowest cathode segments. Generally, when the cell temperature was increased, also the cell performance increased and the current distributions became more even. That can be explained mainly as an increased air convection and decreased activation overpotentials at the electrodes. The deviations from the even current density distribution were also observed to increase as a function of MeOH concentration, resulting from the increased MeOH crossover rate.

Because the areal variations in the cell current give information of local concentrations of reacting species and other mass-transfer phenomena, the complicated connections between different operating parameters can be clarified in a very convenient way. It can be observed immediately during the fuel cell testing, in which part of the DMFC most of the current is produced, how even the current distribution is, what the current distribution is along the MeOH flow channel and how much the MeOH crossover phenomenon decreases the cell performance locally. That information can be used for fuel cell modelling and it is also valuable from the view point of membrane and electrode development.

Acknowledgements

Dr. Nadia Walsby is thanked for the preparation of the membranes. Financial support for this work from Tekniikan Edistämissäätiö (TES) and the Academy of Finland (206132) is gratefully acknowledged.

References

[1] W. Qian, D.P. Wilkinson, J. Shen, H. Wang, J. Zhang, J. Power Sources 154 (2006) 202.
[2] S.J.C. Cleghorn, C.R. Derouin, M.S. Wilson, S. Gottesfeld, J. Appl. Electrochem. 28 (1998) 663.
[3] J. Stumper, S.A. Campbell, D.P. Wilkinson, M.C. Johnson, M. Davis, Electrochim. Acta 43 (1998) 3773.
[4] C. Wieser, A. Helmbold, E. Gülzow, J. Appl. Electrochem. 30 (2000) 803.
[5] M. Noponen, T. Mennola, M. Mikkola, T. Hottinen, P. Lund, J. Power Sources 106 (2002) 304.
[6] M. Noponen, T. Hottinen, T. Mennola, M. Mikkola, P. Lund, J. Appl. Electrochem. 32 (2002) 1081.
[7] T. Hottinen, M. Noponen, T. Mennola, O. Himanen, M. Mikkola, P. Lund, J. Appl. Electrochem. 33 (2003) 265.
[8] M. Noponen, J. Ihonen, A. Lundblad, G. Lindbergh, J. Appl. Electrochem. 34 (2004) 255.
[9] Z. Liu, Z. Mao, B. Wu, L. Wang, V. Schmidt, J. Power Sources 141 (2005) 205.
[10] X.-G. Yang, N. Burke, C.-Y. Wang, K. Tajiri, K. Shinohara, J. Electrochem. Soc. 4 (2005) 759.
[11] R. Eckl, R. Grinzinger, W. Lehnert, J. Power Sources 154 (2006) 171.
[12] E. Gülzow, T. Kaz, R. Reissner, H. Sander, L. Schilling, M.v. Bradke, J. Power Sources 105 (2002) 261.
[13] R. Liu, E.S. Smotkin, J. Electroanal. Chem. 535 (2002) 49.
[14] M. Mench, Q. Dong, C. Wang, J. Power Sources 124 (2003) 90.
[15] A.B. Geiger, R. Eckl, A. Wokaun, G.G. Scherer, J. Electrochem. Soc. 151 (2004) 394.
[16] D.J.L. Brett, S. Atkins, N.P. Brandon, V. Vesovic, N. Vasileiadis, A. Kucernak, Electrochem. Solid-State Lett. 6 (2003) 63.
[17] G. Bender, T. A. Zawodzinski, Spatial distribution of the CO transient response of a PEFC, in: Proceedings of the Electrochemical Society, vol. 2002–31 (Proton Conducting Membrane Fuel Cells III), Electrochemical Society, Los Alamos National Laboratory, Los Alamos, NM, USA, 2005, pp. 212–219.
[18] A. Heinzel, V. Barrágan, J. Power Sources 84 (1999) 70.
[19] H. Dohle, J. Divisek, R. Jung, J. Power Sources 86 (1999) 469.
[20] H. Dohle, J. Divisek, J. Mergel, H. Oetjen, C. Zingler, D. Stolten, J. Power Sources 105 (2002) 274.
[21] B. Gurau, E.S. Smotkin, J. Power Sources 112 (2002) 339.
[22] J.P.G. Villaluenga, B. Seoane, V.M. Barrágan, C. Ruiz-Bauzá, J. Colloid Interf. Sci. 268 (2003) 476.
[23] S. Sandhu, R. Crowther, J. Fellner, Electrochim. Acta 50 (2005) 3985.
[24] T. Schaffer, T. Tschinder, V. Hacker, J.O. Besenhard, J. Power Sources 153 (2006) 210.
[25] J.P.G. Villaluenga, B. Seoane, V.M. Barrágan, C. Ruiz-Bauzá, J. Membr. Sci. 274 (2006) 116.
[26] V. Silva, A. Mendes, L. Madeira, S. Nunes, J. Membr. Sci. 276 (2006) 126.
[27] X. Ren, T. Springler, T.A. Zawodzinski, S. Gottesfeld, J. Electrochem. Soc. 147 (2000) 466.
[28] T. Kallio, K. Kisko, K. Kontturi, R. Serimaa, F. Sundholm, G. Sundholm, Fuel Cells 4 (2004) 328.
[29] V. Saarinen, T. Kallio, M. Paronen, P. Tikkanen, E. Rauhala, K. Kontturi, Electrochim. Acta 50 (2005) 3453.

[30] V. Saarinen, M. Karesoja, T. Kallio, M. Paronen, K. Kontturi, J. Membr. Sci. 280 (2006) 20.
[31] M. McGovern, P. Waszczuk, A. Wieckowski, Electrochim. Acta 51 (2006) 1194.
[32] R.J. Behm, Z. Jusys, J. Power Sources 154 (2006) 327.
[33] C.-Y. Wang, Chem. Rev. 104 (2004) 4727.
[34] A.Z. Weber, J. Newman, Chem. Rev. 104 (2004) 4679.
[35] K.Z. Yao, K. Karan, K.B. McAuley, P. Oosthuizen, B. Peppley, T. Xie, Fuel Cells 4 (2004) 3.
[36] K. Scott, W. Taama, J. Cruickshank, J. Appl. Electrochem. 28 (1998) 289.
[37] K.-D. Kreuer, J. Membr. Sci. 185 (2001) 29.
[38] J.G. Liu, T.S. Zhao, Z.X. Liang, R. Chen, J. Power Sources 153 (2006) 61.
[39] T. Lehtinen, G. Sundholm, S. Holmberg, F. Sundholm, P. Björnbom, M. Bursell, Electrochim. Acta 43 (1998) 1881.
[40] N. Walsby, F. Sundholm, T. Kallio, G. Sundholm, J. Polym. Sci. Part A: Polym. Chem. 39 (2001) 3008.
[41] N. Walsby, S. Hietala, S. Maunu, F. Sundholm, T. Kallio, G. Sundholm, J. Appl. Polym. Sci. 86 (2002) 33.
[42] M. Hogarth, G. Hards, Pt. Met. Rev. 40 (1996) 155.
[43] H. Dohle, J. Mergel, D. Stolten, J. Power Sources 111 (2002) 268.